

Luminescence, Cathodoluminescence and $\text{Ce}^{3+} \rightarrow \text{Eu}^{2+}$ Energy Transfer and Emission Enhancement in the $\text{Sr}_5(\text{PO}_4)_3\text{Cl}:\text{Ce}^{3+},\text{Eu}^{2+}$ Phosphor

Lei Zhou^a, Hongbin Liang^{a*}, Peter A. Tanner^{a*}, Su Zhang^a, Dejian Hou^a, Chunmeng Liu^a, Ye Tao^b, Yan Huang^b, Lina Li^c

^aMOE Laboratory of Bioinorganic and Synthetic Chemistry, State Key Laboratory of Optoelectronic Materials and Technologies, School of Chemistry and Chemical Engineering, Sun Yat-sen University, Guangzhou 510275, P.R. China

^bBeijing Synchrotron Radiation Facility, Institute of High Energy Physics, Chinese Academy of Sciences, Beijing 100039, P.R. China

^cShanghai Institute of Applied Physics, Chinese Academy of Sciences, Shanghai 201204, P.R. China

Supporting Information

Fig. S1. (a) The X-ray excited emission spectra of BaF_2 crystal and powder samples. (b) X-ray excited emission of BaF_2 and $\text{Sr}_{4.91}\text{Ce}_{0.045}\text{Na}_{0.045}(\text{PO}_4)_3\text{Cl}$ at 295 K.

Fig. S2. Room temperature diffuse reflectance spectra of the $\text{Sr}_5(\text{PO}_4)_3\text{Cl}$ host and doped samples by Ce^{3+} and Eu^{2+} .

Fig. S3. Ultraviolet excitation and emission spectra of $\text{Sr}_{5-2x}\text{Ce}_x\text{Na}_x(\text{PO}_4)_3\text{Cl}$ at room temperature.

Fig. S4. (a) Room temperature ultraviolet emission ($\lambda_{\text{ex}} = 288 \text{ nm}, 343 \text{ nm}$) and excitation ($\lambda_{\text{em}} = 443 \text{ nm}$) spectra of $\text{Sr}_{5-x}\text{Eu}_x(\text{PO}_4)_3\text{Cl}$, $x = 0.001$.

Fig. S5. XANES spectra of $\text{Sr}_{5-x}\text{Eu}_x(\text{PO}_4)_3\text{Cl}$, $x = 0.02$ and 1, and comparison with Eu_2O_3 and $\text{BaMgAl}_{10}\text{O}_{17}:\text{Eu}^{2+}$.

Fig. S6. The ultraviolet emission and excitation spectra of $\text{Sr}_{4.98}\text{Ce}_{0.01}\text{Na}_{0.01}(\text{PO}_4)_3\text{Cl}$ (i, black line), $\text{Sr}_{4.98}\text{Eu}_{0.02}(\text{PO}_4)_3\text{Cl}$ (ii, red line) and $\text{Sr}_{4.96}\text{Ce}_{0.01}\text{Eu}_{0.02}\text{Na}_{0.01}(\text{PO}_4)_3\text{Cl}$ (iii, blue line) at 295 K.

Fig. S7. The luminescence decay curves of $\text{Sr}_{4.98}\text{Ce}_{0.01}\text{Na}_{0.01}(\text{PO}_4)_3\text{Cl}$, $\text{Sr}_{4.98}\text{Eu}_{0.02}(\text{PO}_4)_3\text{Cl}$ and $\text{Sr}_{4.96}\text{Ce}_{0.01}\text{Eu}_{0.02}\text{Na}_{0.01}(\text{PO}_4)_3\text{Cl}$ at 295 K.

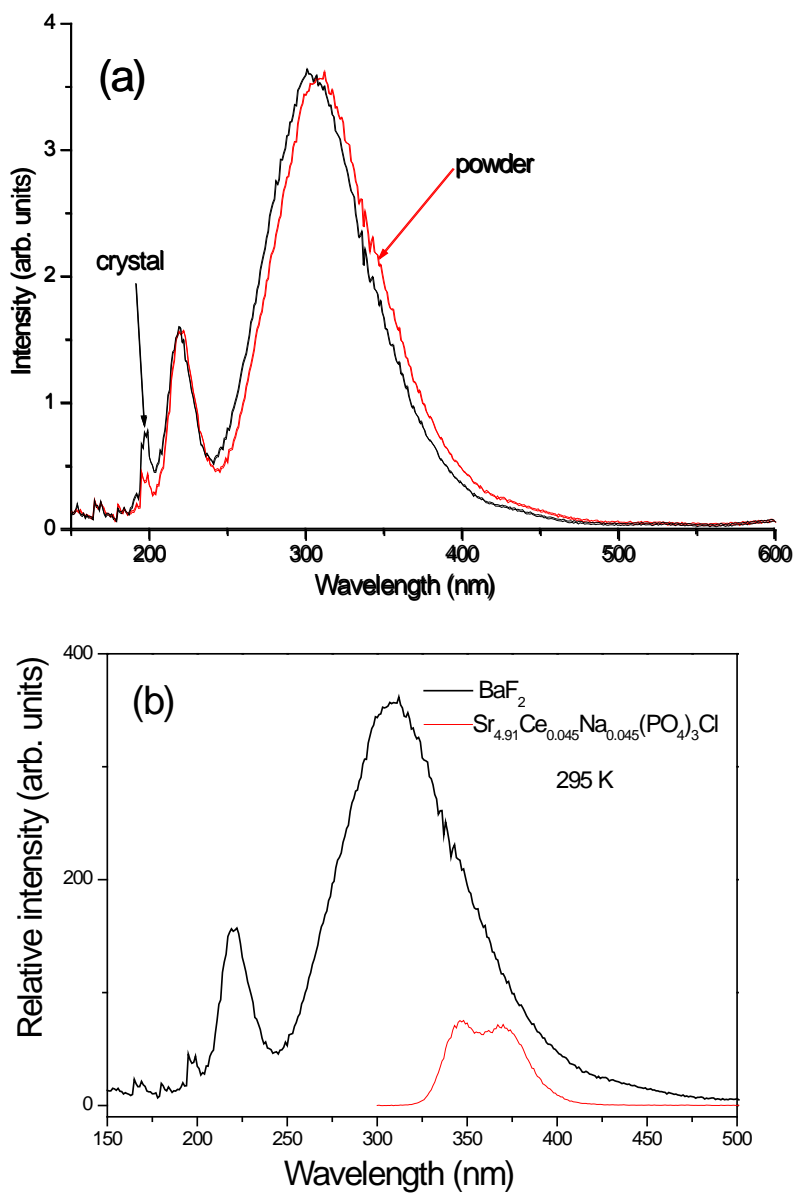
Fig. S8. Time-resolved emission spectra of $\text{Sr}_{4.96}\text{Ce}_{0.01}\text{Eu}_{0.02}\text{Na}_{0.01}(\text{PO}_4)_3\text{Cl}$ at 295 K. A F900 lamp (150 W) was employed as excitation source with a pulse width of 1 ns and pulse repetition rate of 40–100 kHz.

Fig. S9. The luminescence decay curves of $\text{Sr}_{4.98-x}\text{Ce}_{0.01}\text{Eu}_x\text{Na}_{0.01}(\text{PO}_4)_3\text{Cl}$ ($x = 0.001 - 0.50$) at 295 K.

Fig. S10. Room temperature spectral overlap of normalized Ce^{3+} emission and Eu^{2+} absorption in $\text{Sr}_5(\text{PO}_4)_3\text{Cl}$.

Fig. S11. Effect of accelerating voltage and current density upon the intensity of Eu^{2+} cathodoluminescence of singly and doubly-doped $\text{Sr}_5(\text{PO}_4)_3\text{Cl}$ and BAM.

Fig. S1. (a) The X-ray excited emission spectra of BaF₂ crystal and powder samples. (b) X-ray excited emission of BaF₂ and Sr_{4.91}Ce_{0.045}Na_{0.045}(PO₄)₃Cl at 295 K.



X-ray excited luminescence spectra were recorded with a Philips PW2253/20 X-ray tube with a Cu anode operating at 60 kV and 25 mA. A 3 mm aluminum filter was used to cut off soft X-rays. The slit width was fixed at 1 mm and a resolution of 2.1 nm was employed. The emission

of the sample was dispersed by means of an Acton Research Corporation (ARC) VM-504 monochromator, with a 1200 groove mm^{-1} grating blazed at 300 nm and detected by a Hamamatsu R943-02 photomultiplier tube. All spectra were corrected for the wavelength dependence of the photomultiplier quantum efficiency as well as for the monochromator transmission. With this method, the wavelength integrated emission intensity provides a relative estimate for the total light yield. The absolute total light yield of BaF_2 ($8880 \text{ photon (MeV)}^{-1}$) was obtained and was used as a reference. Because all phosphors are powder samples pressed into a pellets, the X-ray excited emission of a powder pellet and crystalline BaF_2 sample were measured to obtain the ratio between powder pellet and crystal light yield (see [Fig. S1\(a\)](#)).

The 195 nm and 220 nm peaks in (a) are attributed to core valence luminescence. The peak at about 310 nm is due to self-trapped exciton emission and the small rise at 440 nm indicates a second order transmission of the 220 nm peak. By comparing the integral light yield measured for a powder pellet with that measured for BaF_2 with identical experimental parameters an estimate for the absolute scintillation yield under X-ray excitation is thus obtained. The average ratio between the integrated emission of a powder pellet and the crystalline BaF_2 sample is 0.99. These are estimates and errors of $\pm 30\%$ are well possible.

The spectrum of $\text{Sr}_{4.91}\text{Ce}_{0.045}\text{Na}_{0.045}(\text{PO}_4)_3\text{Cl}$ ([Fig. S1\(b\)](#)) shows a broad emission band peaking at 347, 370 nm attributed to $\text{Ce}^{3+} 5d \rightarrow 4f$ emission, in line with the positions observed in [Fig. S3](#). The absolute yield was calculated as 600 photons/MeV of absorbed X-ray energy for the sample, which is much smaller than that of commercial scintillators and not suitable for scintillator applications.

Fig. S2. Room temperature diffuse reflectance spectra of the $\text{Sr}_5(\text{PO}_4)_3\text{Cl}$ host and doped samples by Ce^{3+} and Eu^{2+} .

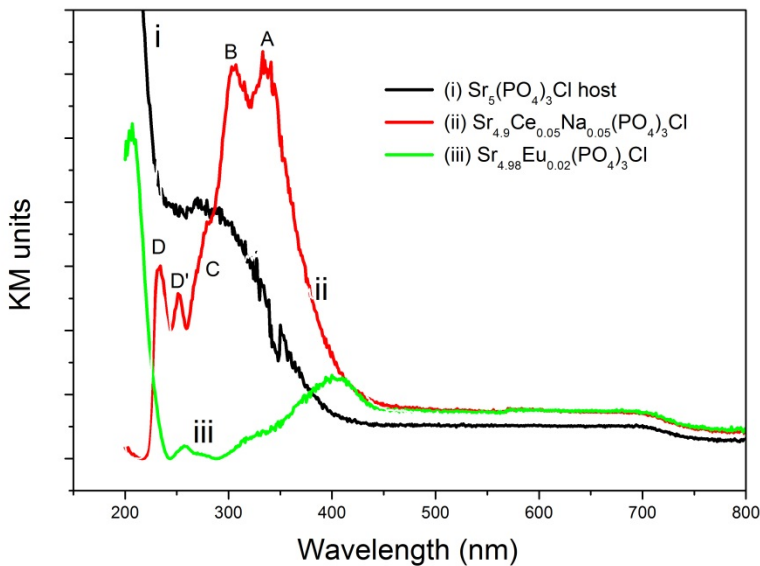


Fig. S3. Ultraviolet excitation and emission spectra of $\text{Sr}_{5-2x}\text{Ce}_x\text{Na}_x(\text{PO}_4)_3\text{Cl}$ at room temperature.

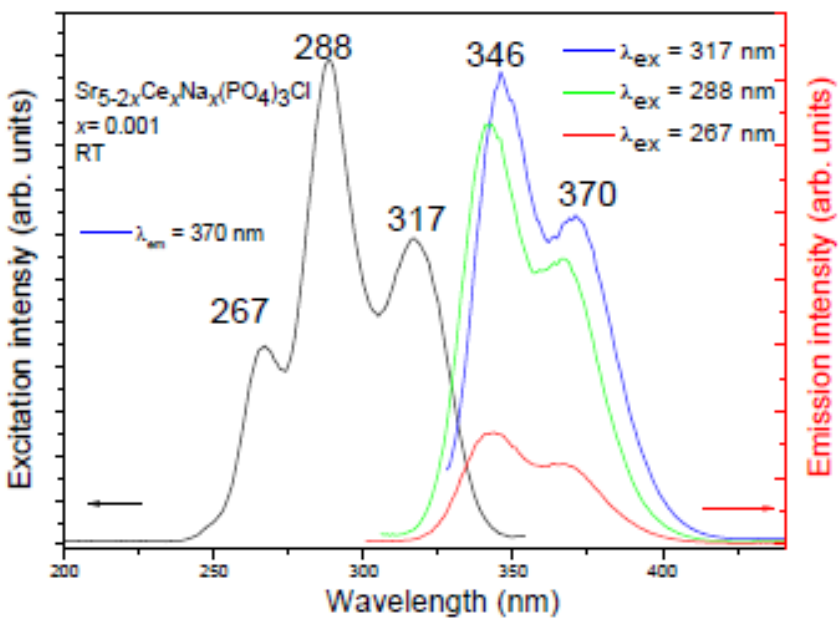


Fig. S4. (a) Room temperature ultraviolet emission ($\lambda_{\text{em}} = 288$ nm, 343 nm) and excitation ($\lambda_{\text{em}} = 443$ nm) spectra of $\text{Sr}_{5-x}\text{Eu}_x(\text{PO}_4)_3\text{Cl}$, $x = 0.001$. The emission spectra are normalized by maximum peak heights.

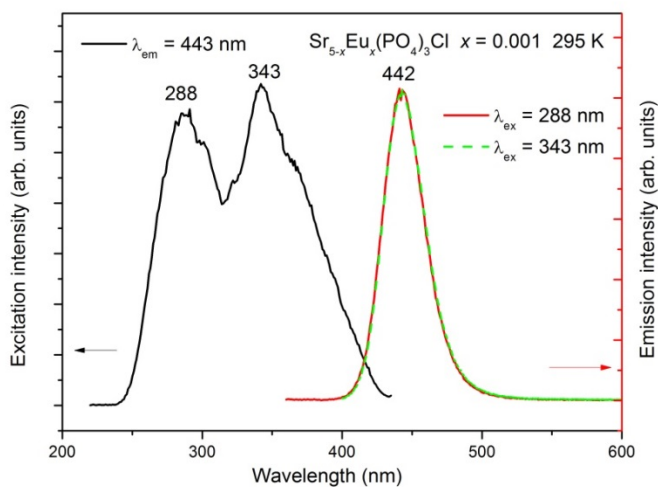


Fig. S5. XANES spectra of $\text{Sr}_{5-x}\text{Eu}_x(\text{PO}_4)_3\text{Cl}$, $x = 0.02$ and 1, and comparison with Eu_2O_3 and $\text{BaMgAl}_{10}\text{O}_{17}:\text{Eu}^{2+}$.

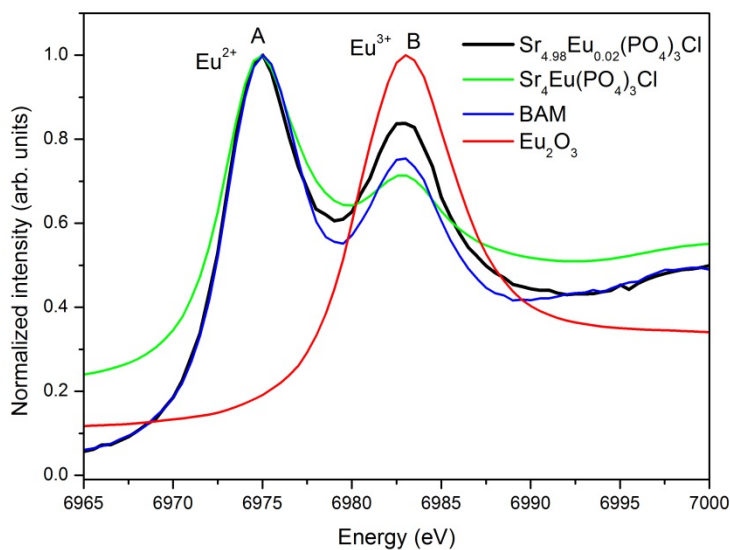


Fig. S6. The ultraviolet emission and excitation spectra of $\text{Sr}_{4.98}\text{Ce}_{0.01}\text{Na}_{0.01}(\text{PO}_4)_3\text{Cl}$ (i, black line), $\text{Sr}_{4.98}\text{Eu}_{0.02}(\text{PO}_4)_3\text{Cl}$ (ii, red line) and $\text{Sr}_{4.96}\text{Ce}_{0.01}\text{Eu}_{0.02}\text{Na}_{0.01}(\text{PO}_4)_3\text{Cl}$ (iii, blue line) at 295 K.

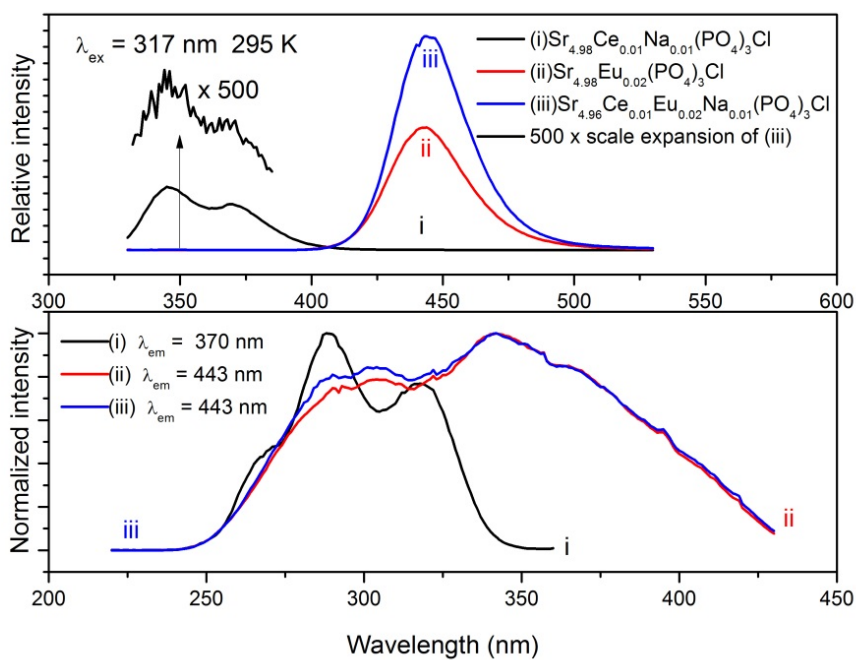


Fig. S7. The luminescence decay curves of $\text{Sr}_{4.98}\text{Ce}_{0.01}\text{Na}_{0.01}(\text{PO}_4)_3\text{Cl}$, $\text{Sr}_{4.98}\text{Eu}_{0.02}(\text{PO}_4)_3\text{Cl}$ and $\text{Sr}_{4.96}\text{Ce}_{0.01}\text{Eu}_{0.02}\text{Na}_{0.01}(\text{PO}_4)_3\text{Cl}$ at 295 K.

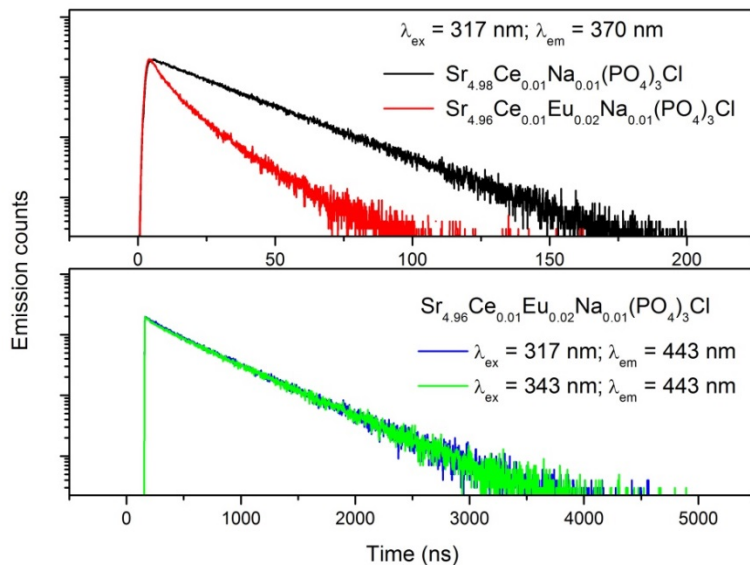


Fig. S8. Time-resolved emission spectra of $\text{Sr}_{4.96}\text{Ce}_{0.01}\text{Eu}_{0.02}\text{Na}_{0.01}(\text{PO}_4)_3\text{Cl}$ at 295 K. A F900 lamp (150 W) was employed as excitation source with a pulse width of 1 ns and pulse repetition rate of 40–100 kHz.

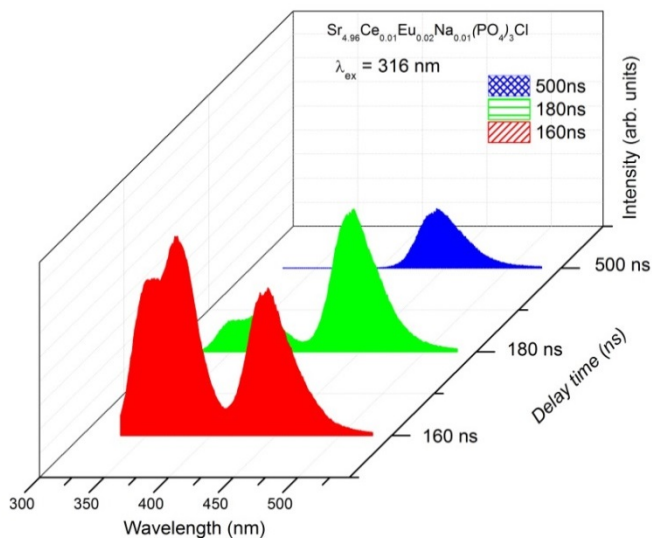


Fig. S9. The luminescence decay curves of $\text{Sr}_{4.98-x}\text{Ce}_{0.01}\text{Eu}_x\text{Na}_{0.01}(\text{PO}_4)_3\text{Cl}$ ($x = 0.001 - 0.50$) at 295 K.

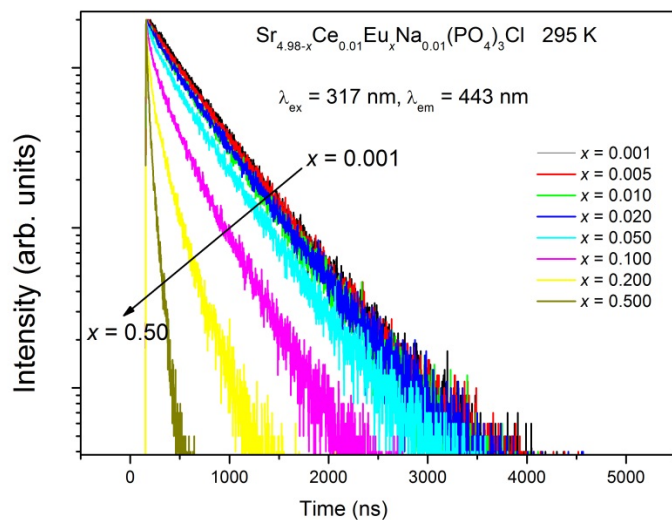


Fig. S10. Room temperature spectral overlap of normalized Ce^{3+} emission and Eu^{2+} absorption in $\text{Sr}_5(\text{PO}_4)_3\text{Cl}$.

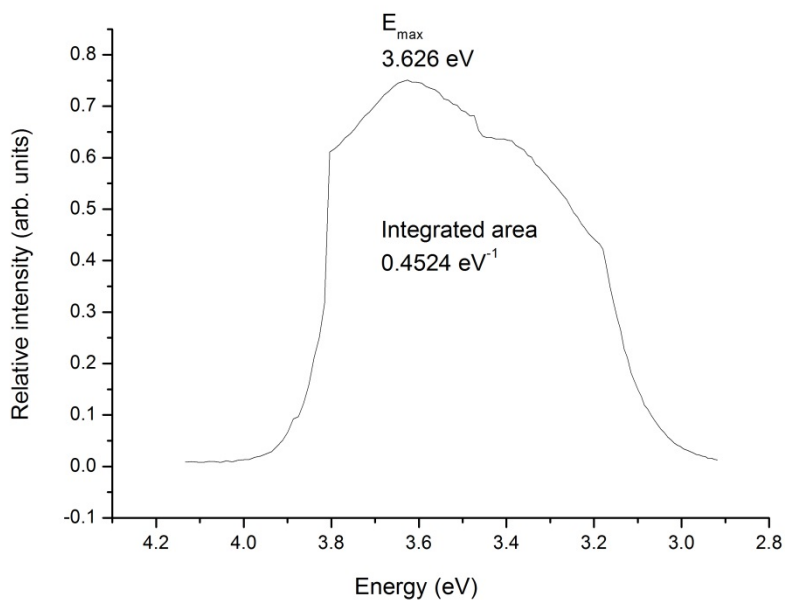


Fig. S11. Effect of accelerating voltage and current density upon the intensity of Eu^{2+} cathodoluminescence of singly and doubly-doped $\text{Sr}_5(\text{PO}_4)_3\text{Cl}$ and BAM.

